O'Hagan, M. P., Ramos-Soriano, J., Haldar, S., Sheikh, S., Morales, J. C., Mulholland, A. J., & Galan, M. C. (2020). Visible-light photoswitching of ligand binding mode suggests G-quadruplex DNA as a target for photopharmacology. *Chemical Communications*, *56*(38), 5186-5189. https://doi.org/10.1039/D0CC01581D

COMMUNICATION

Visible-light photoswitching of ligand binding mode suggests G-quadruplex DNA as a target for photopharmacology

Received 00th January 20xx,
Accepted 00th January 20xx

DOI: 10.1039/x0xx00000x

Michael P. O'Hagan,[a] Javier Ramos-Soriano,[a] Susanta Haldar,[a,b] Sadiyah Sheikh,[a] Juan C. Morales,[c] Adrian J. Mulholland,[a,b] M. Carmen Galan*[,a]

We report the selective targeting of telomeric G4 DNA with a dithienylethene ligand and demonstrate the robust visible-light mediated switching of the G4 ligand binding mode and G-tetrad structure in physiologically-relevant conditions. The toxicity of the ligand to cervical cancer cells is modulated by the photoisomeric state of the ligand, indicating for the first time the potential of G4 to serve as a target for photopharmacological strategies.

Stimuli-driven regulation of biomolecule/ligand complexes is a powerful tool for the control of biological function and a potential source of new tools for chemical biology, nanotechnology, material sciences, pharmacology and medicine.[1] Light is an attractive means for the control of responsive systems, since it can be administered with spatiotemporal precision in a highly controlled, non-invasive manner.[2] In particular, a there is burgeoning interest in controlling the biological activity of molecules with light as the basis of new therapeutic strategies.[3–5] Such photopharmacological approaches are attractive, since they allow more localised control of the therapeutic activity, thereby reducing or eliminating off-target effects. G-quadruplexes (G4) are a class of four-stranded nucleic acid secondary structures formed from guanine-rich sequences that have demonstrated significant potential a therapeutic target in a range of disease classes.[6] Despite the significance of G4 as a therapeutic target, the opportunity to exploit G4 as a photopharmacological target has not yet been explored. Previous attempts to influence G4 ligand activity with light[7,8] have limited applicability in biological circumstances since their effects are hampered in physiological conditions containing high concentrations of metal ions, and they generally rely on high-energy ultraviolet light to effect the photoresponse, which is toxic to cells and unable to penetrate biological matter.[4] We reasoned that many of these limitations could be circumvented by a more judicious choice of ligand chromophore with inherently superior photoresponsive properties. Dithienylethene (DTE)[9,10] is a well-studied photoresponsive scaffold (Figure 1a). Whilst the binding of a small number of these derivatives to duplex DNA oligomers[11,12] and calf-thymus DNA[13] has briefly been investigated by others, the potential of this scaffold to serve as the basis of photoresponsive and selective G4 binding ligand had not yet been explored. Herein, we demonstrate that a pyridinium-decorated DTE ligand selectively targets G4 with discrimination against duplex DNA. For the first time, the ligand binding mode to different G4 topologies can be controlled in a practical, robust and reversible manner using low-energy visible light sources. We further show that the cytotoxicity of the molecule towards HeLa cancer cells is influenced by its photoisomeric state. These results indicate the potential of photoresponsive G4 ligands to serve as the basis of new photopharmacological agents.

We synthesized pyridinium ligand **1o** (Figure 1a) through a straightforward 4-step procedure (ESI, Scheme S1). We first verified that the reported photochromic properties of the ligand were maintained in conditions relevant to G4 folding, namely 100 mM sodium phosphate buffer, pH 7.4. Pleasingly, reversible photoswitching between the open (**1o**) and closed (**1c**) isomers was observed under these conditions by alternate irradiation with 450 nm and 635 nm visible light (Figure 1b). The presence of clear isosbestic points indicate clean photoisomerization between the two forms of the ligand, and the photogeneration of the **1c** isomer was also demonstrated by NMR (ESI, Figure S1).

To assess the ligand selectivity for G4 and as a first step towards examining the differences between the two photoisomeric forms of the ligand on G4 binding, we conducted FRET thermal melting assays of **1o**/**1c** against fluorophore-labelled G4 (F21T) and duplex DNA (F10T) models. In this study the ligand-induced stabilisation of the secondary DNA structure is observed by the change in apparent melting temperature (ΔT_m) of the folded species (see ESI for full details).[14] The results (Figure 2 and ESI, Tables S1-S2) confirm the selectivity of the ligands for the G4 DNA sequence over the duplex model. Most notably, ligand **1c** appears most active against the G4 sequence in potassium-containing buffer (ΔT_m = 13 °C at 10 μM ligand concentration) whilst duplex stabilisation remains very low (ΔT_m < 1 °C) under

[a] School of Chemistry, University of Bristol, Cantock's Close, Bristol BS81TS, UK
[b] Centre for Computational Chemistry, University of Bristol, UK
[c] Department of Biochemistry and Molecular Pharmacology, Instituto de Parasitología y Biomedicina López Neyra, CSIC, PTS Granada, Avda. del Conocimiento, 17, 18016 Armilla, Granada, Spain
Electronic Supplementary Information (ESI) available. See DOI: 10.1039/x0xx00000x

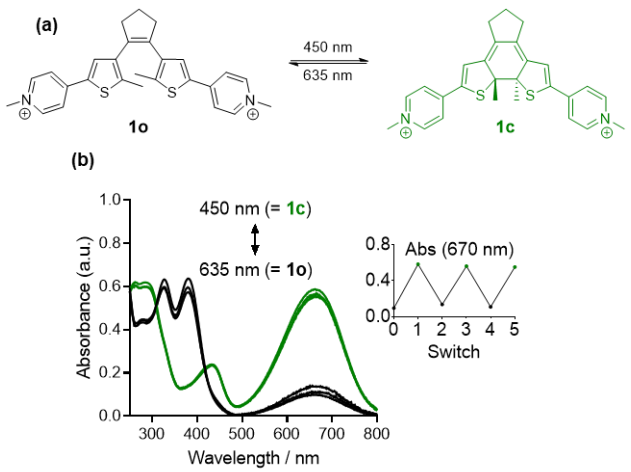

Figure 1. (a) Dithienylethene ligand couple **1o** (black) and **1c** (green) studied in this work; (b) photoswitching between **1o**/**1c** states in 100mM sodium phosphate buffer, monitored by UV-visible spectroscopy, [ligand] = 50 µM. The inset shows the reversible switching over several cycles by monitoring absorbance at 670 nm.

comparable conditions. Importantly, greater thermal stabilisation (ESI, Figure S2) is induced by the **1c** isomer (ΔT_m = 13 °C) than the **1o** form (ΔT_m = 10 °C). Though this difference appears modest, control experiments revealed significant thermal cyclo-reversion of **1c** to **1o** occurs at temperatures close the melting temperature of the G4 (ESI, Figure S3). The thermal stabilisation induced by **1c** is therefore likely depressed by back-isomerisation to **1o** isomer under the experimental conditions. Despite this, it appears that **1c** photoisomer is the more active form of the ligand. The induced thermal stabilisation of the G4 sequence in sodium-containing buffer remains evident (ΔT_m = 4 °C) confirming the overall G4/duplex selectivity, but is likely too low for differences in the activity of the two isomers **1o** and **1c** against F21T to be observed under sodium-rich conditions. The dependence of the ligand activity on the metal ion likely results from the influence of the cation on the overall G4 structure. As discussed further below, sodium generally favours an antiparallel G4 fold, whilst a hybrid topology is adopted in the presence of potassium. These different 3-dimensional structures therefore give rise to the possibility of different interaction modes with the same ligands.

To examine the differences in G4 binding mode between the two forms of the photochromic ligand in more detail, we undertook ^{1}H NMR studies supported by circular dichroism spectroscopy and UV-visible spectroscopy. We first selected the telo22 sodium structure for our structural investigations, since it folds into a single well-characterized antiparallel G4 conformation, allowing facile assignment of many of the imino and aromatic resonances from simple 1D ^{1}H spectra (Figure 3a and ESI, Figure S4-S8).[15] Striking differences in ligand binding mode were observed between ligands **1o** and **1c**. The closed form **1c** causes significant perturbations to the chemical shifts of imino resonances (Figure 3b): G8 is shifted significantly upfield whilst several aromatic proton resonances corresponding to the top G-tetrad and lateral loops are also perturbed, particularly G8 and G20 (Figure 3c and ESI, Figure S5). Significant shifts can also be observed for imino protons G22 and G14 corresponding to the lower G-tetrad (Figure 3b), implying that ligand **1c** binds with a 2:1 stoichiometry to the upper and lower faces of the G4. Meanwhile, ligand **1o** does not significantly change the chemical shifts of the imino protons (Figure 3d and ESI, Figure S7) but does induce specific perturbations of residues A7 and T18 (Figure 3e) corresponding to the capping residues of the lateral loops above the top G-tetrad. That all residues of the lower G-tetrad are unperturbed suggests that ligand **1o** binds exclusively to the top of the G4 with 1:1 stoichiometry, in contrast to **1c** which associates with both upper and lower G-tetrads. These results indicate that **1o** and **1c** associate to antiparallel G4 with different binding modes and stoichiometry, with the closed form **1c** stacking onto the terminal G-tetrads (resulting in the observed perturbations of the imino resonances) whilst the open form **1o** remains external to the top of the G4, associating with the terminal capping residues. Cartoon representations of the proposed binding modes are shown in Figures 3f and 3g). Molecular dynamics studies also indicate that **1o** to interacts primarily with T18 and A7 external to the G4 (ESI, Figure S9a). The tetrad-stacking mode of **1c** was not directly observed in the time course of the simulation, but the ligand-induced breakage of the hydrogen bond between A19 and T6 is indicative that the capping residues open on ligand binding, allowing access to the G-tetrad in the longer time courses required to reach the equilibrium binding mode observed in the experimental study (ESI, Figure S9b). UV-visible titration studies (assuming the stoichiometry indicated in the NMR experiments) indicated similar apparent dissociation constants of K_d = (6 ± 1) µM for **1o** and (7 ± 1) µM for **1c** (ESI, Figures S10-S11). The apparent similar affinity of the two binding modes corroborates the FRET results which indicate that **1o** and **1c** induce the same thermal stabilisation to F21T in sodium containing buffer (Figure 2). Critically, the two distinct binding modes of the ligand were reversibly switched by alternate irradiation with blue (450 nm) and red (635 nm) visible light, monitored by following the chemical shift of the G8 and G4 imino protons upon ligand isomerisation (ESI, Figure S12). No photodegratation of the underlying oligonucleotide was observed during this process, a distinct advantage arising from the avoidance of high-energy UV light sources. To the best of our knowledge, the **1o**/**1c** system provides the first example of

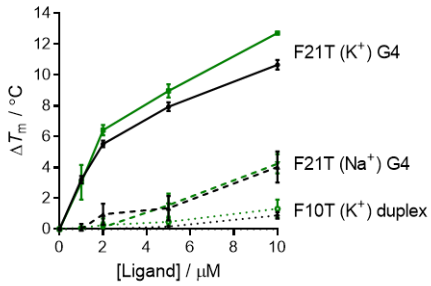

Figure 2. Induced thermal stabilization ($\Delta T_{1/2}$) by **1o** (black) and **1c** (green) of F21T G4 and F10T duplex sequences monitored by the FRET melting assay.

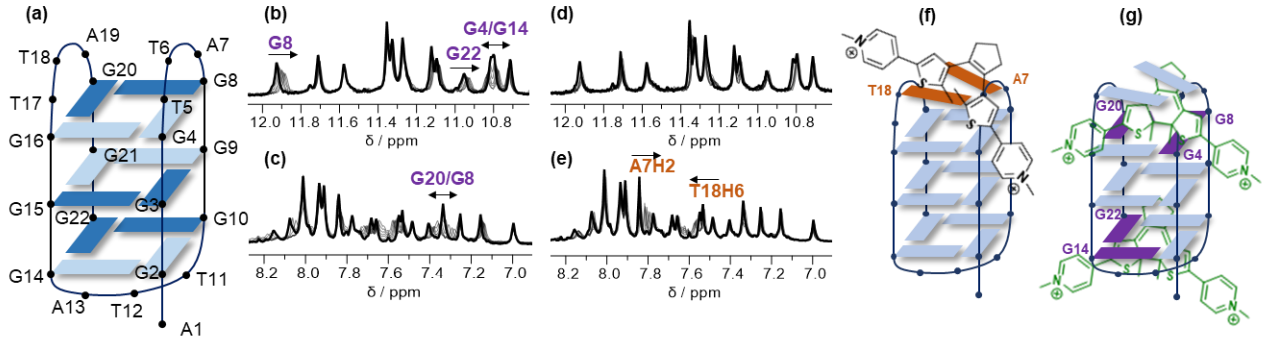

Figure 3. NMR investigations of the binding modes of **1o**/**1c** to antiparallel telo22 DNA. (a) cartoon representation of the antiparallel fold showing base numbering. (b)-(e): Superimposed imino (b),(d) and aromatic (c),(e) NMR spectra of telo22 and increasing concentrations of (b),(c) **1c** and (d),(e) **1o**.[18] (f)-(g) putative ligand binding poses modes of (f) **1o** and (g) **1c** to telo22 DNA based on the observed chemical shift perturbations.

the bistable photoresponsive control of G4 ligand binding mode.

Encouraged by these results, we continued our study by investigating the effect of ligands **1o** and **1c** on the telo23 hybrid form of G4 DNA (Figure 4a and ESI, Figure S13-S18)[16] which has greater physiological relevance owing to the higher concentration of potassium ions in cellular environments.[17] As in the case of the antiparallel telo22 G4, the closed isomer **1c** causes significant chemical shift perturbations (Figure 4b) of the imino signals of several guanine residues, indicative of efficient stacking with the exposed G-tetrads. Again, since signals corresponding to both upper (G9/G21) and lower (G15/G23) tetrads are perturbed, we infer a 2:1 ligand binding stoichiometry in this case. The intensity of the imino signals is maintained throughout the titration and the circular dichroism spectrum of the oligonucleotide is unaffected (ESI, Figure S16a) indicating that the binding of **1c** takes place without disruption of the hybrid G4 fold. In sharp contrast, ligand **1o** induces the pronounced attenuation of many of the G4 imino signals, particularly G9, G10, G21 and G22 (Figure 4b). Indeed, only a small number of distinctive imino environments can be seen in the spectrum of the telo23/**1o** complex, rather than the 12 signals expected for a fully-folded G4 (if present as a single species). This indicates that the binding of the open form **1o** requires partial disruption of the G-tetrad network, pointing to an intercalative binding mechanism. Indeed, while the CD spectrum of telo23 is unperturbed by the addition of ligand **1c** (*vide supra*), the addition of **1o** results in attenuation of ellipticity from 240-280 nm, corroborating the disruption of the native G-tetrad network by addition of ligand (ESI, Figure S16b) observed by NMR. It is interesting that binding of ligand **1o** appears to disrupt the native G4 structure, given that the results of the thermal melting assay indicate **1o** confers thermal stability to G4. However, the loss of stability expected due to partial perturbation of the G-tetrad network may be compensated by favourable interactions with the ligand in an intercalated structure. Furthermore, the ligand concentrations required for NMR experiments (200 μM) are significantly higher than those employed in the FRET assay (10 μM). Despite the clear differences observed in the NMR and CD titrations, similar apparent disassociation constants (K_d ≈ 6 μM for both **1o** and**1c**) were obtained for the two photoisomeric ligand forms in UV-visible titration studies (ESI, Figure S19-S20). Whilst it could be possible for the different binding modes to have similar overall affinities, it should be noted that the obtained binding constants are only apparent values and should be interpreted with caution owing to the complex nature of G4/ligand interactions and ligand-induced structural perturbation. These factors may result in more complex association mechanisms than the classical host-guest equilibria assumed in the derivation of the binding models. The ligand binding mode and accompanying disruption/regeneration of the G-tetrad structure could be controlled reversibly by alternate irradiation with blue and red light. The switching process could be achieved at least seven times, monitored by NMR, with no observable degradation of the underlying DNA structure (Figures 4c and ESI, Figure S21). The degree of structural perturbation was controlled by varying the irradiation time and measured by the integral of the G9/G10 envelope. Recovery of the of G-tetrad network upon irradiation of the **1o**/telo23 complex was also confirmed by CD spectroscopy (Figure 4d). Faster response times could easily be achieved by employing brighter irradiation sources, but the slower kinetics observed with the low power (4.5 mW) light source used in this study are helpful for demonstrating that the extent of structural perturbation can be controlled simply by varying the irradiation dose, and that even mild irradiation sources are sufficient to exert control over the present system.

Towards our goal of examining the potential of the photoresponsive G4 ligand as a photopharmacological agent, we undertook toxicity assays of **1o**/**1c** in HeLa cervical cancer cells (Figure 5). A two-fold difference in cytotoxic activity between the isomers is clearly observed (IC_{50} **1o** = 23 μM, **1c** 10 μM), thereby indicating that the toxic effect of the pyridinium-DTE scaffold is dependent on the photoisomeric form of the ligand. It is noteworthy that the IC_{50} values are comparable to the G4 affinity observed in the biophysical studies, indicating G4-binding as a plausible mechanism of action of the **1o**/**1c** couple, though alternative therapeutic mechanisms cannot be unambiguously discounted at this stage. To the best of our knowledge, this is the first time a G4 ligand derived from a molecular photoswitch has shown potential as a

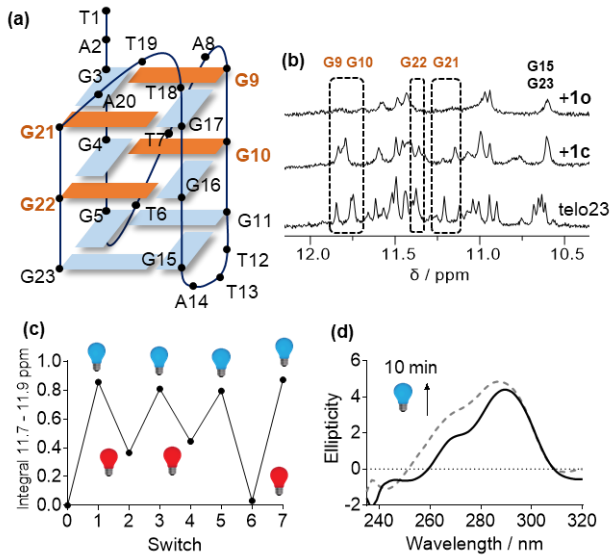

Figure 4. NMR and CD investigations of the binding modes of **1o**/**1c** to hybrid telo23 DNA (a) cartoon representation of the hybrid fold showing base numbering. The highlighted bases indicate the tetrad regions disrupted on binding ligand **1o** (b) stacked NMR spectra showing perturbations of telo23 imino resonances by **1c** and loss of imino resonances by **1o.** (c) reversible switching of tetrad disruption/reformation by alternative blue/red light irradiation quantified by the by normalized integral over the range 11.7-11.9 ppm. (d) CD spectra of telo23 (4.2 μM) and 100 μM **1o** before (solid black trace) and after (dotted grey trace) 10 min irradiation with 450 nm light showing recovery of G4 band intensity indicative of G-tetrad reformation on isomerisation of **1o** to **1c**.

photopharmacological agent in vitro. Further work to probe the detailed mechanism of action **1o**/**1c** is underway in light of these promising results.

In conclusion, we have demonstrated an example of a photoresponsive dithienylethene ligand that targets G4 in preference to duplex DNA. The binding mode of the ligand to G4 can be regulated practically in a bidirectional manner with low-energy, biologically-compatible visible light sources. To the best of our knowledge, this is the first example of a G4 ligand that can be controlled in this manner. The observed control of ligand binding mode (telo22) and G-tetrad formation (telo23) suggests a variety of possible applications of DTE derivatives in the development of responsive G4/ligand systems. Towards one such application, we have shown that the toxicity of the ligand can be is dependent on the photoisomeric state, thereby indicating G4 ligands have the potential to serve as the basis of new photopharmacological agents. Given the ever-increasing focus on G4-targeting therapy and the more recent emergence of the field of photopharmacology, we believe this proof-of-concept study makes a key connection that will serve to develop advances in both these fields. Further studies into optimising the potency and difference in biological activity of visible-light responsive G4 ligands are under active exploration in our laboratory and will be reported in due course.

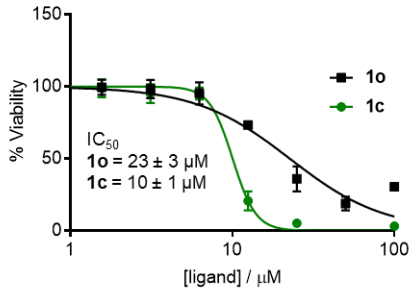

Figure 5. Viability assay data for ligands **1o**/**1c** against HeLa cells after 72h incubation

Conflicts of interest

There are no conflicts to declare.

Acknowledgements

MPO thanks the Bristol Chemical Synthesis Centre for Doctoral Training, funded by EPSRC (EP/L015366/1) and the University of Bristol, for a PhD studentship, JRS acknowledges a MSCA fellowship (project 843720-BioNanoProbes). S.H. and A.J.M. thanks EPSRC for support [grant numbers EP/M015378/1 and EP/M022609/1]. This work was carried out using the computational facilities of the Advanced Computing Research Centre, University of Bristol - http://www.bris.ac.uk/acrc/ S.S. thanks the Bristol Centre For Functional Nanomaterials (EPSRC EP/L016648/1). JCMS thanks the Spanish Ministerio de Economía y Competitividad (Grant CTQ2015-64275-P and RTI2018-099036-B-I00). MCG thanks the European Research Council (ERC-COG: 648239).

Notes and references

1 F. Wang, X. Liu and I. Willner, *Angew. Chemie - Int. Ed.*, 2015, **54**, 1098–1129.
2 A. S. Lubbe, W. Szymanski and B. L. Feringa, *Chem. Soc. Rev.*, 2017, **46**, 1052–1079.
3 W. A. Velema, W. Szymanski and B. L. Feringa, *J. Am. Chem. Soc.*, 2014, **136**, 2178–2191.
4 M. M. Lerch, M. J. Hansen, G. M. van Dam, W. Szymanski and B. L. Feringa, *Angew. Chemie - Int. Ed.*, 2016, **55**, 10978–10999.
5 J. Broichhagen, J. A. Frank and D. Trauner, *Acc. Chem. Res.*, 2015, **48**, 1947–1960.
6 S. Neidle, *J. Med. Chem.*, 2016, **59**, 5987–6011.
7 M. P. O'Hagan, S. Haldar, M. Duchi, T. A. A. Oliver, A. J. Mulholland, J. C. Morales and M. C. Galan, *Angew. Chemie Int. Ed.*, 2019, **58**, 4334–4338.
8 X. Wang, J. Huang, Y. Zhou, S. Yan, X. Weng, X. Wu, M. Deng and X. Zhou, *Angew. Chemie - Int. Ed.*, 2010, **49**, 5305–5309.
9 F. Hu, L. Jiang, M. Cao, Z. Xu, J. Huang, D. Wu, W. Yang, S. H. Liu and J. Yin, *RSC Adv.*, 2015, **5**, 5982–5987.
10 M. Herder, B. M. Schmidt, L. Grubert, M. Pätzel, J. Schwarz and S. Hecht, *J. Am. Chem. Soc.*, 2015, **137**, 2738–2747.
11 K. Liu, Y. Wen, T. Shi, Y. Li, F. Li, Y. L. Zhao, C. Huang and T. Yi, *Chem. Commun.*, 2014, **50**, 9141–9144.
12 A. Mammana, G. T. Carroll, J. Areephong and B. L. Feringa, *J. Phys. Chem. B*, 2011, **115**, 11581–11587.
13 T. C. S. Pace, V. Müller, S. Li, P. Lincoln and J. Andréasson, *Angew. Chemie - Int. Ed.*, 2013, **52**, 4393–4396.
14 A. De Cian, L. Guittat, M. Kaiser, B. Saccà, S. Amrane, A. Bourdoncle, P. Alberti, M. P. Teulade-Fichou, L. Lacroix and J. L. Mergny, *Methods*, 2007, **42**, 183–195.
15 Y. Wang and D. J. Patel, *Structure*, 1993, **1**, 263–282.
16 K. N. Luu, A. T. Phan, V. Kuryavyi, L. Lacroix and D. J. Patel, *J. Am. Chem. Soc.*, 2006, **128**, 9963–9970.
17 O. S. Andersen, in *Encyclopedia of Metalloproteins*, eds. R. H. Kretsinger, V. N. Uversky and E. A. Permyakov, Springer, New York, 2013.
18 Assignment of A7H2 is tentative owing to overlap with the A1H2 signal in the absence of ligand, see ESI for further details.